TURBINE BLADE VIBRATION UNDER VARIABLE SPEED OPERATION

by

V. Selvam

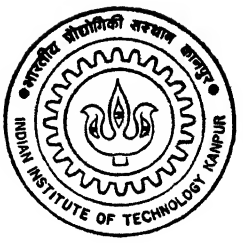

DEPARTMENT OF MECHANICAL ENGINEERING

INDIAN INSTITUTE OF TECHNOLOGY KANPUR

FEBRUARY, 1996

TURBINE BLADE VIBRATION UNDER VARIABLE SPEED OPERATION

A Thesis Submitted

in Partial Fulfilment of the Requirements

for the Degree of

MASTER OF TECHNOLOGY

by

V.SELVAM

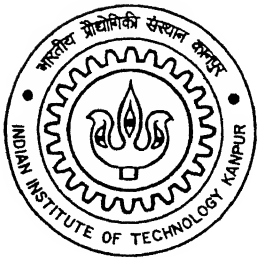

to the

DEPARTMENT OF MECHANICAL ENGINEERING

INDIAN INSTITUTE OF TECHNOLOGY KANPUR

FEBRUARY, 1996

CERTIFICATE

It is certified that the work contained in this thesis, entitled **"Turbine Blade Vibration Under Variable Speed Operation"**, by V Selvam, has been carried out under my supervision and that this work has not been submitted elsewhere for a degree

Nalinaksh S. Vyas
Associate Professor
Department of Mechanical Engineering
Indian Institute of Technology
Kanpur

February, 1996.

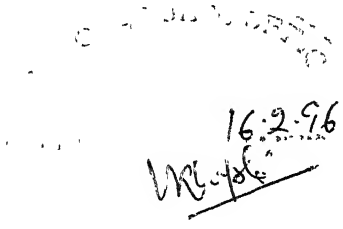

ACKNOWLEDGEMENTS

I express my deep gratitude to Dr.N S Vyas, my thesis supervisor, for his valuable guidance and constant encouragement throughout this work I have the highest regards for his openness to discussions, patience towards my riders, granting freedom to work independently and constructive criticism from time to time Working with him has indeed been an enriching experience for me

I express my thanks to Mr M.M Singh, who have been supportive throughout.

I gratefully acknowledge the help rendered by Mr A A Khan, Mr.D A Jeyaraj and Mr S Ravi towards the preparation of this document

I wish to express thanks to all my friends in I I.T , Kanpur, who have shared my joys and sorrows during this course.

V.SELVAM

Indian Institute of Technology, Kanpur.

February, 1996.

CONTENTS

NOMENCLATURE

A	*Area of cross-section*
A_i , B_i ...F_i	*Arbitrary parameters in shape functions*
B_i	*Body force distribution*
a,b	*Coefficients in trigonometric series of forcing functions*
C	*Torsional stiffness*
$[C]$	*Damping matrix*
C_v	*Proportional damping coefficient*
E	*Modulus of Elasticity*
e	*Engineering normal strain*
F_x, F_y	*Forcing functions*
f_i , g_i, h_i	*Shape function for bending deflections*
H	*Dynamic Magnification Factor (Displacement ratio)*
H_{m_k}	*mth harmonic response in the kth mode*
$I_{x_1x_1}$	*Second moment of area about* X_1X_1 *axis*
$I_{y_1y_1}$	*Second moment of area about* Y_1Y_1 *axis*
$I_{x_1y_1}$	*Product moment of area about* X_1Y_1 *axis*
I_{cg}	*Moment of inertia per unit length about centre of gravity*
I_R	*Reissner's functional*
L	*Reissner's dynamic functional*
l	*Blade length*
M	*Moment*
M_x, M_y	*Moment in x and y directions*
m	*Harmonic number; material constant*
n_s	*Number of nozzles*
p_k	*Natural frequency in the kth mode*
Q	*Forcing vector*
R	*Disc radius*
r_0	*Initial nondimensional frequency*
r_i	*Instantaneous nondimensional frequency (frequency ratio)*

r_α	*Nondimensional acceleration (sweep rate)*
r_x, r_y	*Co-ordinates of the center of flexure*
T	*Kinetic energy*
T_q	*Twisting moment*
t	*Time*
$[U]$	*Modal matrix*
U_0^*	*Complementary energy density function*
u_i	*Displacement in the i-th direction*
v	*Volume*
xx, yy	*Coordinate axes through center of flexure*
x_1x_1, y_1y_1	*Coordinate axes through centroid*
XX, YY	*Principal axes*
z	*Distance along the blade length*
α	*Angular acceleration*
$\eta\eta, \xi\xi$	*Co-ordinate axes*
η	*Generalized co-ordinate*
ν	*Nozzle passing frequency*
τ	*Nondimensional time*
ζ	*Modal damping ratio*
ρ	*Mass density*
ω	*Angular frequency*
ω_0	*Initial angular frequency*
ϕ	*Stagger angle*
$(')$	*Denotes differentiation with respect to z*
$(\dot{})$	*Denotes differentiation with respect to t*

LIST OF FIGURES

LIST OF TABLES

CHAPTER 1

INTRODUCTION

Turbomachine blade vibration has been an important technical field for many years Blades in a turbomachine represent the most critical components in the design of rotating machinery With increasing severity in operating environment of future turbomachines, the need for more efficient blade design is essential

A typical blade is pretwisted along its length, has curvature (or camber) in the chordwise direction and varies in thickness along the chord. The cross-sections are generally aerofoil in shape Both the thickness and the curvature varies along the length, but decrease from the root to the end The blade width also changes along the length.

Vibration induced fatigue failure of blades is a problem of major concern in turbomachine blading The behaviour of most blades is strongly influenced by the mean and alternating stresses experienced during the operation, by the applied loading history, by the elastic and fatigue properties of the blade and by the operating environment. The critical aspect of the problem constitutes resonant vibration at an integral order speed when the principal component of the vibrating modes in the spinning blade matches both in time and space a corresponding pattern in the gas/steam stream , caused by any distortion in the flow field. This may give rise to large dynamic stresses leading to fatigue failure. The practice of tuning the blade away from natural frequencies may not always be possible in an engine of advanced design with as many as thousand blades of different characteristics As compared to typical steam turbine power generating systems, with heavy rotors and low operating ranges of speeds, the nature of the problem becomes more apparent for high performance gas turbines operating in supersonic regimes containing several critical speeds The blades get excessively stressed not only during operation of the rotor at constant speeds, but also during their transit past several criticals during acceleration and deceleration operations of the turbomachine In this study, the problem of the determination of transient resonant stresses, during variable speed operations like start-up and shut-down of the machine, is addressed

available unsteady force components and checked his results experimentally. Hoyniak and Fleeter [1981] made an energy balance between unsteady aero-dynamic work and energy dissipation due to aerodynamic damping to predict blade resonant vibrations by employing experimental unsteady aerodynamic gust data for flat chamber cascade airfoils Jadwani and Rao [1982], analyzed the force vibration response using the equations of Lagrange They designed an experimental rig [1982] simulating nozzle by permanent magnets and measured the tip deflection of the rotating blades under nozzle excitation Hiroyuki Kojima [1985] considered the case of forced vibration of a beam with a mass subjected to alternating electro-magnetic force and solved the governing partial differential equations by harmonic balance method Leung [1983] used the dynamic stiffness method relating the amplitude of applied forces and response of a harmonically vibrating continuum damping was incorporated along with load distribution and equivalence of the solution to Duhamel's integral was illustrated. Comparison was made with modal analysis method.

Mac Bain [1976] used finite difference method to determine the transient response of a cantilever plate subjected to normal impact by a ballistic pendulum Sisto and Chang [1981] considered the gyroscopic forces on the dynamic behavior of rotating blades, Coriolis forces were included in the analysis of Sisto, Chang and Sutcu [1982].They also investigated the instabilities due to harmonic variation with time of the processional rate due to whirling and other causes Irretier [1984], using beam theory and modal approximation technique, presented a numerical modal for an untwisted blade to obtain transient vibration response due to partial admission during a change of rotational speed Bannerjee and Kennedy [1985] derived the theoretical expressions for the displacement response of an axially loaded beam subjected to concentrated or distributed loads having stationary and ergodic properties

While considerable amount of activity is witnessed in obtaining the forced vibration response of blades under constant operational speeds of the rotor, transient resonant stress analysis during variable speed operations has not been able to receive any significant attention Such an analysis is of considerable importance for aircraft turbine blading, which experience frequent changes in rotor speed, during various manoevours of the aircraft

1.2 Present Work

In the present study an attempt has been made to develop a procedure for estimation of turbine blade stresses during typical variable speed turbine operations like start-up and shut down. Initially, the response of a single degree of freedom mass-spring-dashpot model, to an external force, with a time dependent excitation frequency, is obtained. For ease of analysis, the excitation

frequency is taken to vary uniformly with time The response is obtained through the use of Duhamel's Integral The response is obtained for different values of damping ratios for various frequency sweep rates, in non-dimensional form The analysis is then extended to the case of an actual turbine blade Using beam theory, neglecting higher order effects such as shear deformation, rotary inertia, Coriolis forces etc , the kinetic energy and the Reissner's functional for a typical tapered, twisted, asymmetric aerofoil cross-section blade mounted at a stagger angle on a disc under rotational acceleration have been derived. Available periodic excitation data , simulating nozzle excitation, is used in Fourier form in the traction forces term of the Reissner's functional Ritz process has been employed to obtain the equations of forced motion. The eigenvalue problem is solved to obtain the free vibration characteristics Modal Analysis technique is then used to decouple the equations of motion The nondimensional response obtained for the single degree of freedom system, is processed with the modal equations of the blade to obtain the transient resonant stresses inflicted on the blade during the variable speed operation of the turbomachine Results are obtained for typical acceleration rates and compared with the corresponding resonant stresses for constant speed operations

CHAPTER 2

RESPONSE OF A SINGLE DEGREE FREEDOM SYSTEM WITH VARIABLE FREQUENCY EXCITATION FORCE

The response of a single degree freedom, mass-spring-dashpot system, to an excitation force with frequency varying with time is analysed, in this chapter. The variation in the excitation frequency is taken to be constant with time, for ease of analysis. Such an analysis is essential, prior to analysing the turbine blade - firstly to understand the phenomenon of a momentarily experienced resonance and secondly, to overcome the computational problems, described in the next chapter, posed by the turbine blade calculations

2.1 Equation of motion and response

Consider a single degree freedom system as shown in Fig 2 1 with an excitation force, $F(t)$, such that at any instant of time, the instantaneous excitation frequency, ω, can be expressed as

$$\omega = \omega_0 + \alpha t \tag{2 1}$$

The instantaneous force is

$$F(t) = F_0 \sin\left(\omega_0 t + \frac{1}{2}\alpha t^2\right) \tag{2 2}$$

ω_0 is the initial excitation frequency, α is the sweep rate or acceleration. The magnitude F_0, of the excitation force is assumed to be constant. (A cosine excitation can be readily accommodated in the above expressions by including appropriate phase angle within the sine excitation force term.)

The equation of motion can be written as

$$m\ddot{x} + c\dot{x} + kx = F_0 \sin\left(\omega_0 t + \frac{1}{2}\alpha t^2\right). \tag{2 3}$$

The above equation of motion does not have an exact analytical solution Reference can be made to Baker [1939], for a graphical method of obtaining the response A numerical procedure is adopted in the present study.

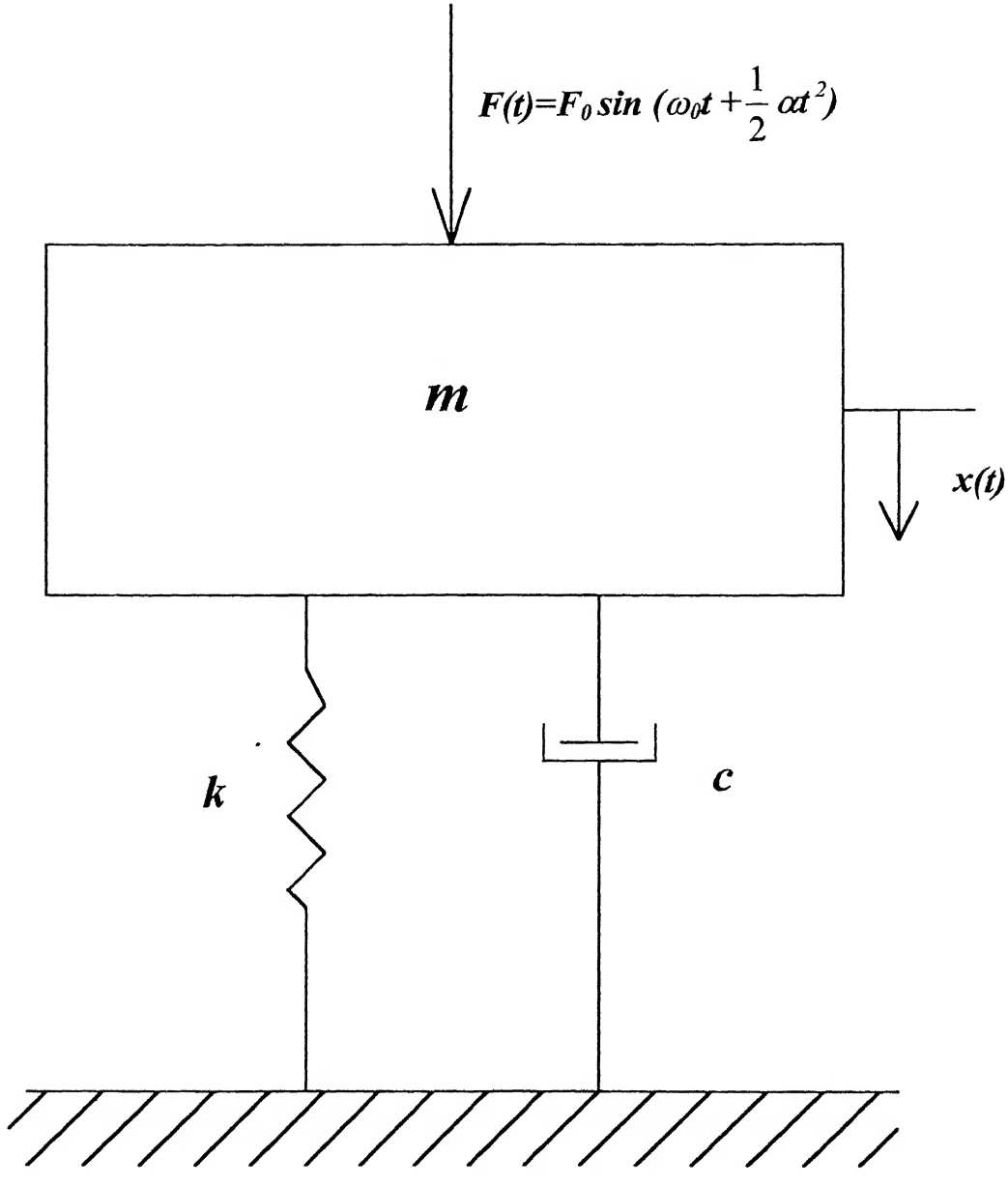

Fig. 2.1 **Single degree of freedom system with variable frequency excitation.**

Defining the following non-dimensional parameters

$\tau = pt$ = non - dimensional time

$r_0 = \frac{\omega_0}{p}$ = initial frequency ratio

$r_i = \frac{\omega}{p}$ = instantaneous frequency ratio

$r_\alpha = \frac{\alpha}{p^2}$ = nondimensional sweep rate (2 4)

$H = \frac{x(t)}{X_{st}}$ = dynamic magnification factor (or displacenent ratio)

$X_{st} = \frac{F_0}{mp^2}$ = static deflection

equation (2 3) can be written as

$$\frac{d^2H}{d\tau^2} + 2\varsigma\frac{dH}{d\tau} + H = \sin(r_0\tau + \frac{1}{2}r_\alpha\tau^2) \tag{2 5}$$

For zero initial conditions, the response of the system, using Duhamel's Integral, is

$$H(\tau) = \int_0^\tau e^{-\zeta(\tau-\tau')} \sin\sqrt{1-\zeta^2}(\tau-\tau')\sin\left(r_0\tau' + \frac{1}{2}r_\alpha\tau'^2\right) d\tau' \tag{2 6}$$

For $\zeta << 1$ the above becomes

$$H(\tau) = \int_0^\tau e^{-\zeta(\tau-\tau')} \sin(\tau-\tau')\sin\left(r_0\tau' + \frac{1}{2}r_\alpha\tau'^2\right) d\tau' \tag{2.7}$$

2.2 Numerical results

Ten-point Gaussian-quatrature is employed to evaluate the integral in equation (2 7) and the nondimensional response (displacement ratio) is obtained as a function of nondimensional time. Figures 2.2 - 2 5 show the nondimensional response H as a function of the nondimensional instantaneous excitation frequency, r_i $(= r_0 + r_\alpha\tau)$, for various values of sweep rate, r_α, and the damping ratio, ζ.

As is known, for a case when excitation frequency is constant (i.e. $\alpha = 0$), resonance occurs when $\omega = p$ In the absence of damping, infinite amplitude of vibration can be theoretically obtained when $\omega/p = 1\,0$ However it takes time for these amplitudes to build up As observed from Fig.2.2(a), the amplitude of vibration builds up as the instantaneous frequency r_i approaches 1.0 . At $r_i = 1.0$ infinitely large amplitude would have built up, had the system

been allowed to 'dwell' at the point The amplitude of vibration starts building up at this point, but once past $r_i = 1.0$, the post resonance effect comes into play Under these influences, a large but finite amplitude of vibration is obtained, not at $r_i = 1.0$, but at the instance 'shifted' from $r_i = 1.0$ (e g at $r_i = 1.06$ for $r_\alpha = 0.75 \times 10^{-3}$)

Figure 2 2 depicts the influence of damping ratio on the peak response With a finite amount of damping existing in the system a portion of the energy supplied is dissipated, leaving less energy for building up of vibrational amplitudes and as expected 'resonant' peaks become lower as the damping increases

The influence of the sweep rate on the peak amplitude is shown in Figures 2.3. These figures have been obtained for a constant value of the damping ratio ($\zeta = 0.0025$) It can be observed that for larger values of r_α,the peak amplitude get reduced and are shifted further from $r_i = 1.0$ For larger r_α, the transit being faster, the energy supplied is utilized more in accelerating the system than in building up vibrational amplitudes Figs 2.4 and 2 5 show similar results for negative rates of acceleration

The peak responses for various positive and negative sweep rates, for various damping values, including those from Figs. 2.2 - 2.5 have been compiled in Table 2 1

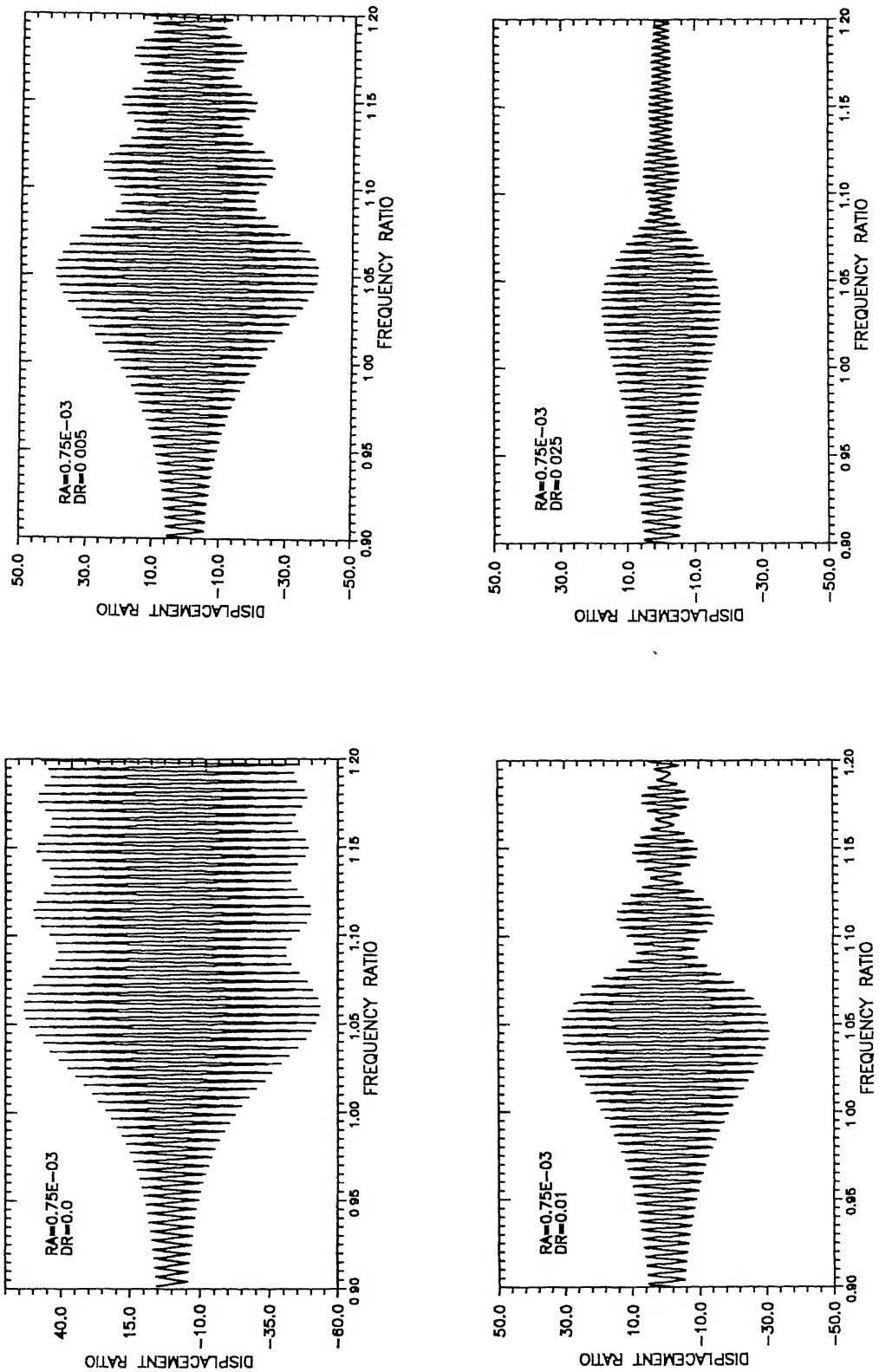

Fig. 2.2 Response under acceleration-Influence of damping ($r_\alpha = 0.75 \times 10^{-3}, r_0 = 0.0$)

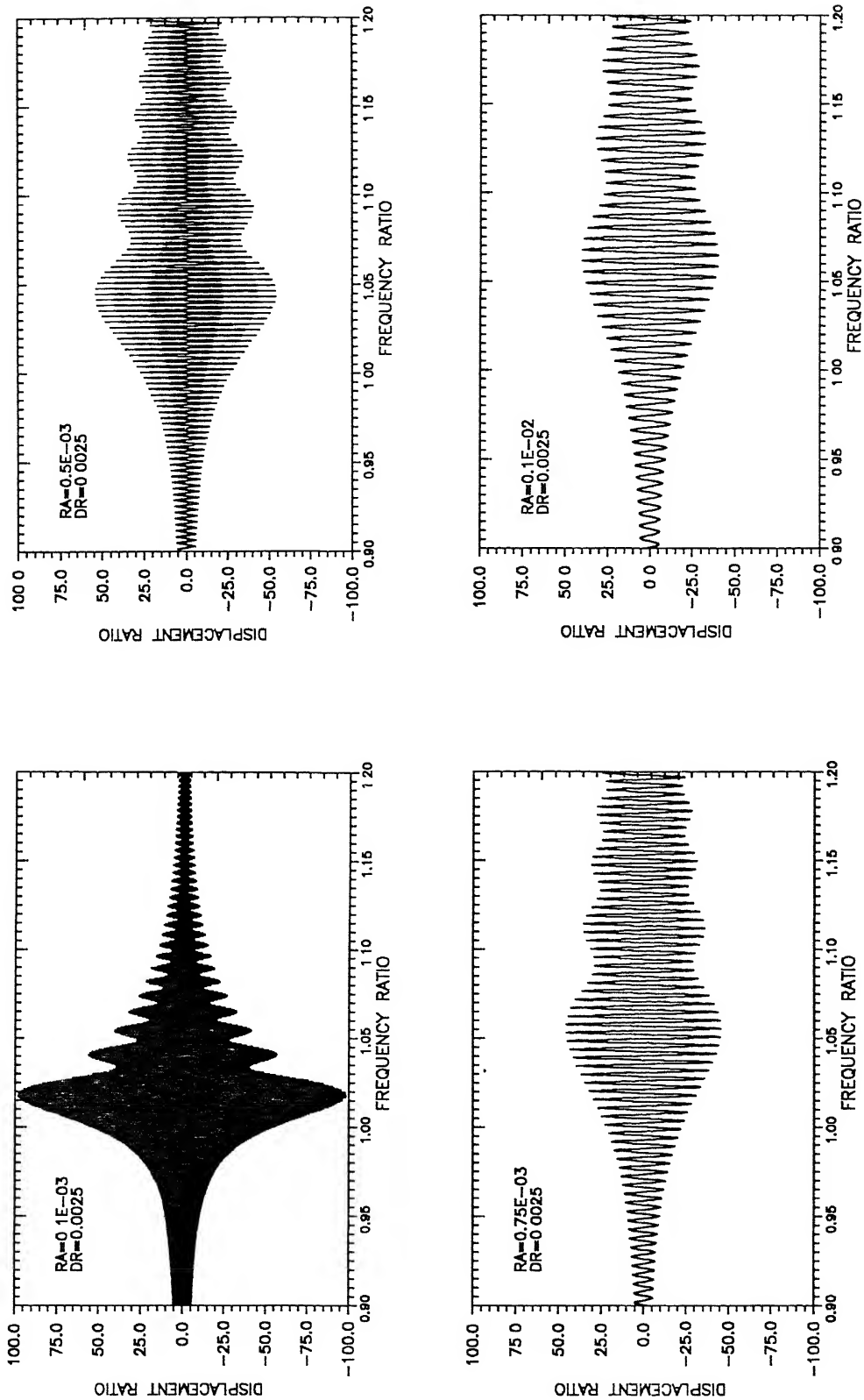

Fig. 2.3 Response under acceleration- Influence of the rate of acceleration

($\zeta = 0.0025$, $r_0 = 0.0$).

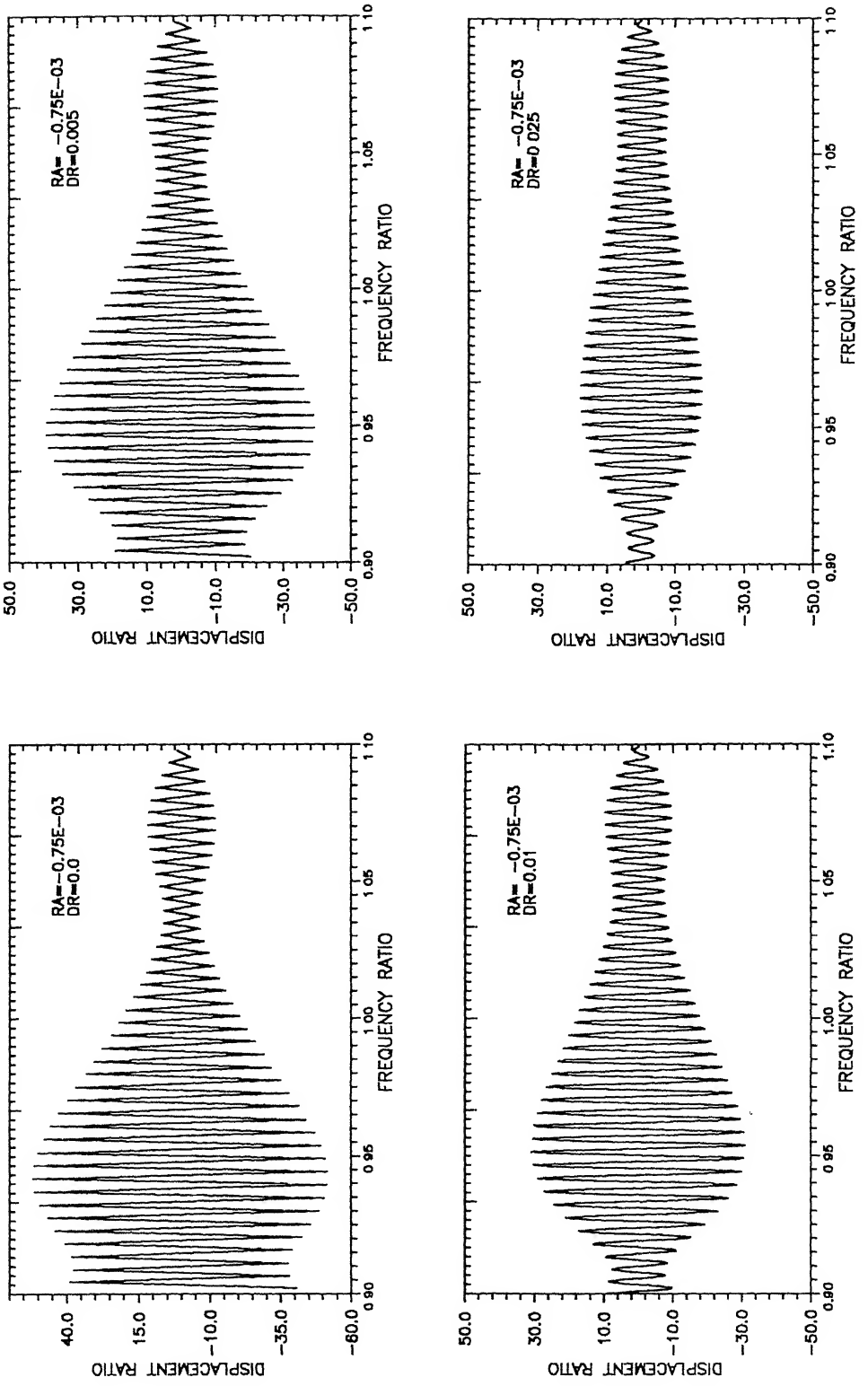

Fig. 2.4 Response under deceleration- Influence of damping ($r_\alpha = -0.75 \times 10^{-3}, r_0 = 1.1$)

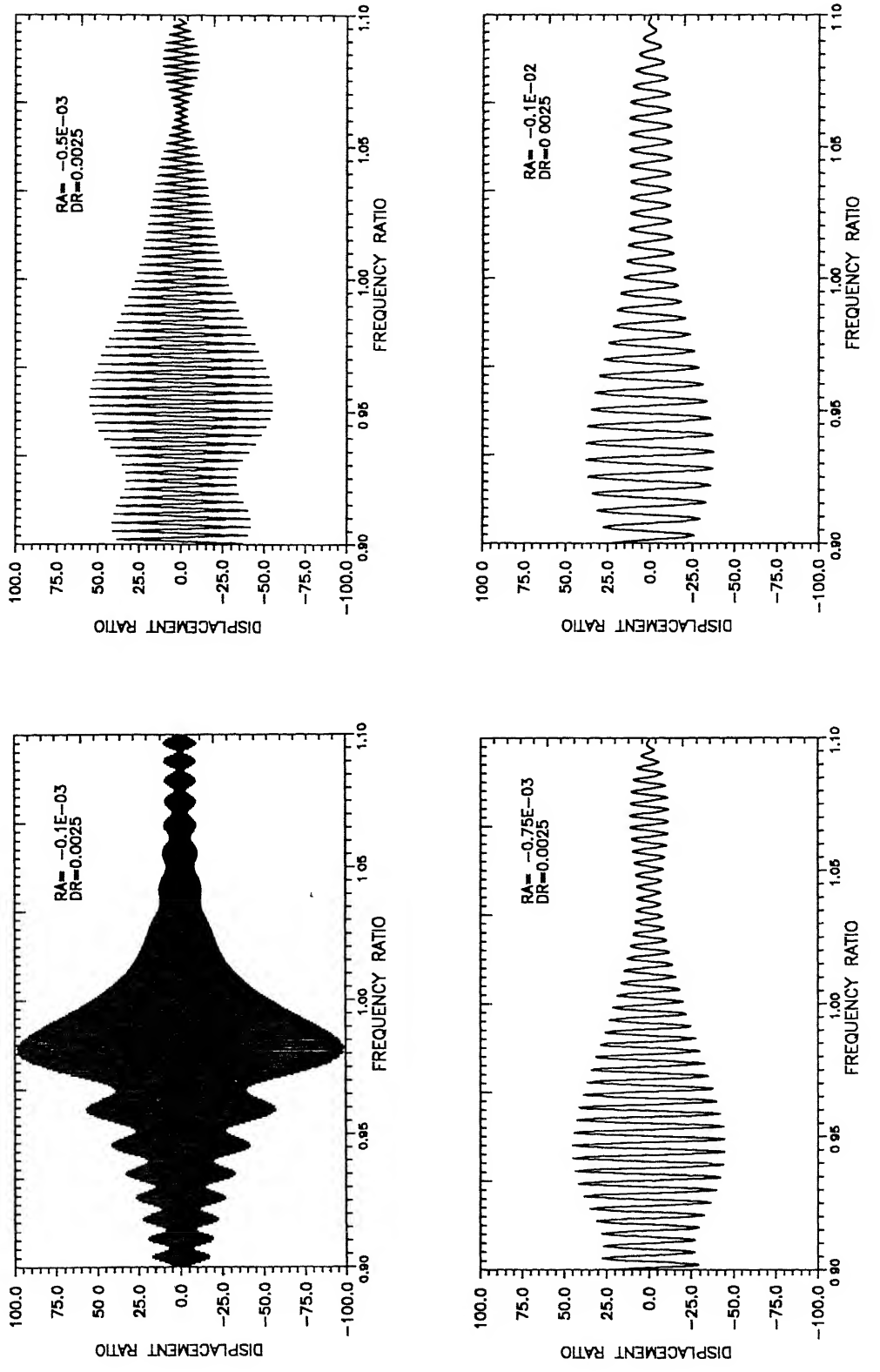

Fig. 2.5 **Response under deceleration- Influence of the rate of deceleration** ($\zeta = 0.0025$ $r_0 = 1.1$).

TABLE 2.1. Maximum Dynamic Magnifications.

	MAXIMUM DYNAMIC MAGNIFICATION, H_{max}									
ACCELERATION	*Damping Ratio*									
RATES	*0.005*	*0.010*	*0.015*	*0.020*	*0.025*	*0.030*	*0.035*	*0.040*	*0.045*	*0.050*
0.25E-04	89 754	48.823	33.079	24 930	19 974	16 653	14 277	12 493	11 104	9 993
0.50E-04	82 111	47 575	32 589	24 767	19 912	16 626	14 264	12 486	11.100	9.991
0.75E-04	76 308	46.171	32 278	24 553	19 825	16 586	14 244	12 475	11.094	9.987
0.10E-03	71.558	44.818	31.893	24.372	19 720	16 536	14.218	12.461	11.086	9 982
0.25E-03	55.001	39.005	29.329	23.357	19 188	16 179	13 988	12 328	11.002	9.931
0.50E-03	49.060	35.585	27 423	22.097	18 492	15 782	13 701	12 093	10 823	9 809
0.75E-03	42 431	32 263	25.650	21.107	17 770	15 356	13 461	11.939	10 698	9 678
0.10E-02	36 907	29 172	23.726	19 871	16 998	14.844	13.112	11.696	10.526	9 555
0.25E-02	21 731	18 893	16 702	14.846	13.268	12.001	10.951	10.033	9 228	8.518
0.50E-02	12 706	11 847	11 064	10 348	9 694	9 096	8 547	8 044	7.582	7.157
- 0.25E-04	89 909	48 978	33 079	24 930	19.974	16.653	14.277	12 493	11 104	9 993
- 0.50E-04	82.414	47.730	32 744	24.767	19.912	16 626	14 264	12 486	11 100	9 991
- 0.75E-04	76.667	46.330	32 431	24 626	19.824	16 587	14 244	12.475	11.094	9.987
- 0.10E-03	72.081	44.992	32.039	24 522	19.740	16 537	14 218	12 461	11 086	9 982
- 0.25E-03	57 438	39.769	29.684	23.534	19.353	16.328	14 089	12.365	11.006	9 931
- 0.50E-03	46 074	34.436	27.056	22 053	18.467	15.841	13.819	12.230	10.942	9 886
- 0.75E-03	39 005	30.823	24.923	20.874	17.735	15 307	13 503	12 029	10 813	9.802
- 0.10E-02	32.220	27.263	23.066	19.644	16.930	14.838	13.148	11 781	10.637	9.680
- 0.25E-02	22.064	19.505	17.345	15 514	13 954	12.619	11 472	10.507	9 700	8.987
- 0.50E-02	12.402	11.624	10.911	10.257	9.656	9.105	8.597	8.129	7 698	7.300

2.3 Remarks

The response data generated in this chapter forms a crucial computational component for obtaining the blade response, described in the next chapter The nondimensional response data of this chapter is employed as a built-in data surface, in the blade program, whereby the blade modal responses are directly extrapolated from this surface

CHAPTER 3

TURBINE BLADE RESPONSE UNDER ACCELERATION

This chapter deals with the forced vibration of a turbine blade, when the turbomachine speed is increased or decreased , as in the step-up and stup-down operations The present analysis is idealized to a case where the rate of change in the rotational frequency of the turbine is constant Reissner's functional, in conjunction with Ritz process has been employed to derive the equations of forced motion The eigenvalue problem is solved to obtain the modal properties and Modal analysis is subsequently carried out to decouple the equations of motion. The results of the previous chapter are then used for a computationally efficient calculation of the modal peak responses The stress response of the blade is computed using Strength of Material formulae.

3.1 Equations of motion

Consider a typical tapered, twisted, asymmetric aerofoil cross-section blade mounted at a stagger angle on a disc rotating with constant acceleration shown in Figs 3 1 and 3.2. The centroid of the cross-section is located at G, while O is the center of flexure. Noting that the general displacement of point P consists of translations about the xx and yy axes and rotation about the centre of flexure, O, the displacements field can be written as

$$\begin{aligned} u_x &= x - y\theta = x_1 - y_1\theta \\ u_y &= y + x\theta = y_1 + x_1\theta \\ u_z &= -x_1 u_x' - y_1 u_y' + u \\ &= -x_1(x_1' - y_{.1}\theta') - y_{.1}(y_1' + x_1\theta') + u \end{aligned} \tag{3.1}$$

The displacement vector U of the particle P can be written as

$$U = PP' = u_x\bar{e}_{x_1} + u_y\bar{e}_{y_1} + u_z\bar{e}_z \tag{3.2}$$

where $\bar{e}_{x_1}, \bar{e}_{y_1}, \bar{e}_z$ denote the rotating unit vectors in x_1, y_1 and z directions respectively The unit vectors $\bar{e}_{x_1}$ and $\bar{e}_{y_1}$ are related to the rotating unit vectors $\bar{e}_\xi$ and $\bar{e}_\eta$ in the ξ and η directions as

$$\begin{aligned} \bar{e}_{x_1} &= \bar{e}_\xi \cos\phi - \bar{e}_\eta \sin\phi \\ \bar{e}_{y_1} &= \bar{e}_\xi \sin\phi + \bar{e}_\eta \cos\phi \end{aligned} \tag{3.3}$$

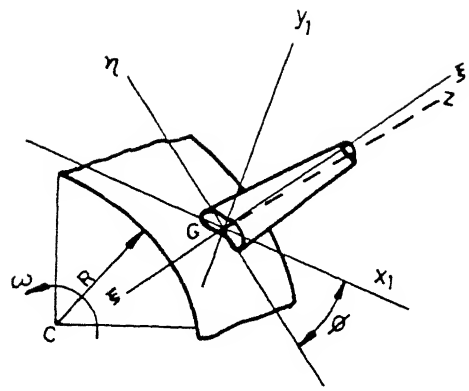

Fig. 3.1 Blade mounted on a rotating disc.

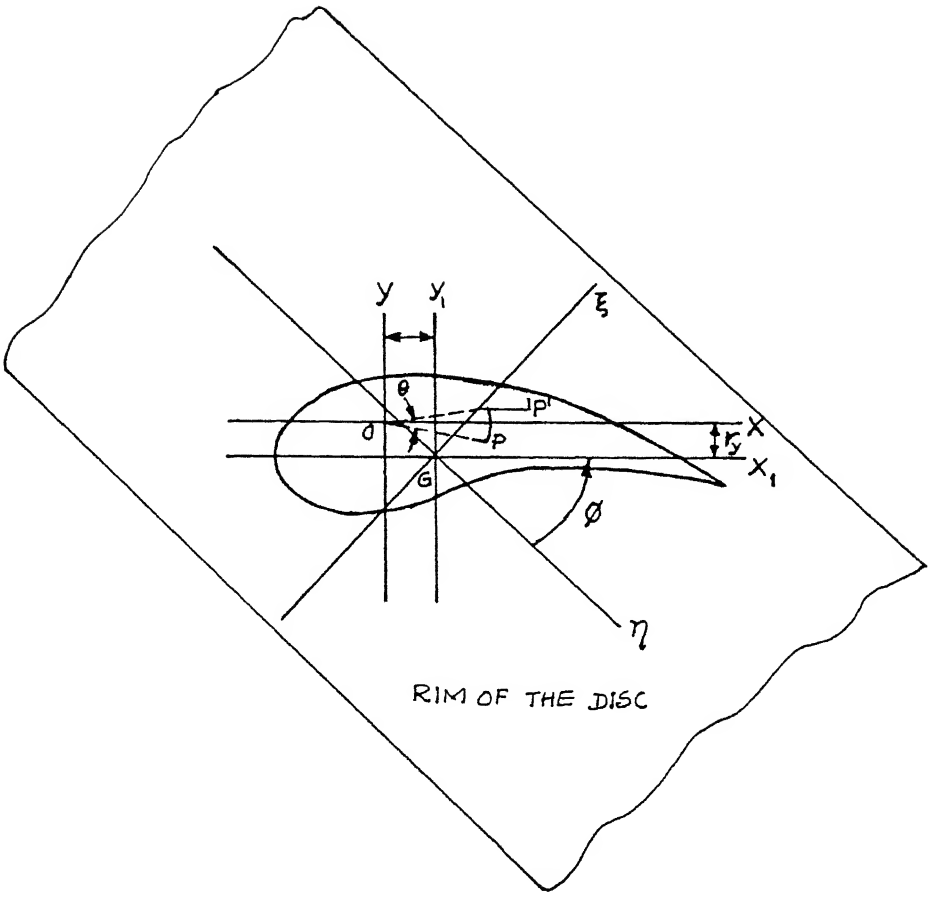

(a) Cross section

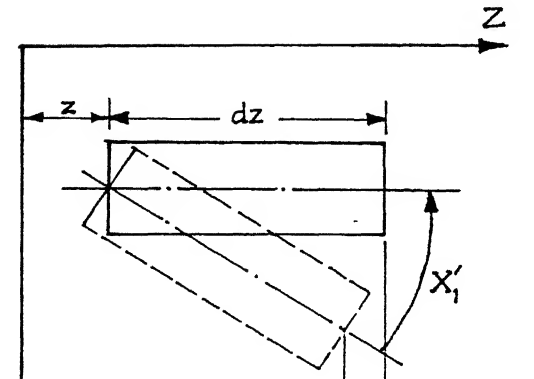

(b) Element rotation in x_1 z plane

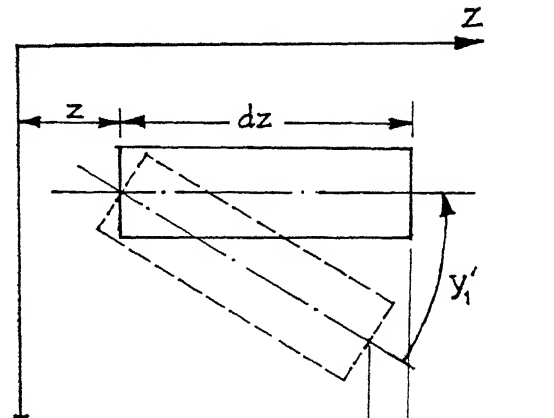

(c) Element rotation in y_1 z plane

Fig. 3.2 Blade cross section.

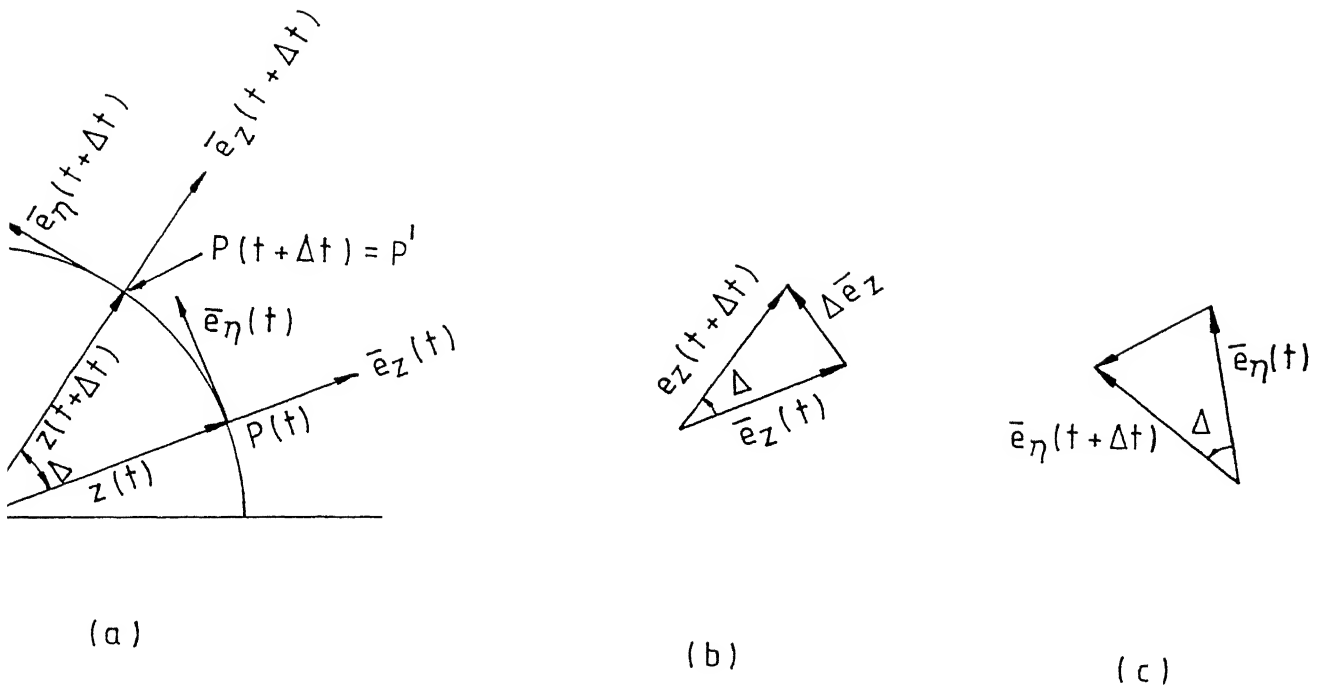

Fig. 3.3 **Rotating vectors.**

Equation (3 2) can be written as

$$U = u_\xi \bar{e}_\xi + u_\eta \bar{e}_\eta + u_x \bar{e}_z \tag{3 4}$$

where the components of displacements u_ξ and u_η in the ξ and η directions are

$$\begin{aligned} u_\xi &= (x_1 - y_1\,\theta)\cos\phi + (y_1 + x_1\,\theta)\sin\phi \\ u_\eta &= -(x_1 - y_1\,\theta)\sin\phi + (y_1 + x_1\,\theta)\cos\phi \end{aligned} \tag{3 5}$$

The position vector of the displaced particle P', from Figs 3 1 and 3 2 is

$$\bar{r} = (R\bar{e}_z) + (\xi \bar{e}_\xi + \eta \bar{e}_\eta + z\bar{e}_z) + (u_\xi \bar{e}_\xi + u_\eta \bar{e}_\eta + u_z \bar{e}_z) \tag{3 6}$$

The above equation can be written as

$$\begin{aligned} \bar{r} &= (\xi + u_\xi)\bar{e}_\xi + (\eta + u_\eta)\bar{e}_\eta + (R + z + u_z)\bar{e}_z \\ &= r_\xi \bar{e}_\xi + r_\eta \bar{e}_\eta + r_z \bar{e}_z \end{aligned} \tag{3 7}$$

Therefore the velocity of the particle is

$$\dot{\bar{r}} = \dot{r}_\xi \bar{e}_\xi + r_\xi \dot{\bar{e}}_\xi + \dot{r}_\eta \bar{e}_\eta + r_\eta \dot{\bar{e}}_\eta + \dot{r}_z \bar{e}_z + r_z \dot{\bar{e}}_z \tag{3.8}$$

Noting from Fig 3.3 that

$$\begin{aligned} \dot{\bar{e}}_z &= \omega \bar{e}_\eta = (\omega_0 + \alpha t)\,\bar{e}_\eta \\ \dot{\bar{e}}_\eta &= -\omega \bar{e}_z = -(\omega_0 + \alpha t)\,\bar{e}_z \\ \bar{e}_\xi &= 0 \end{aligned} \tag{3.9}$$

equation (3 8) becomes

$$\dot{\bar{r}} = \dot{r}_\xi \bar{e}_\xi + (\dot{r}_\eta + \omega r_z)\bar{e}_\eta + (\dot{r}_z - \omega r_\eta)\bar{e}_z \tag{3 10}$$

Hence,

$$\begin{aligned} v^2 &= \dot{\bar{r}} \cdot \dot{\bar{r}} \\ &= (\dot{r}_\xi^2 + \dot{r}_\eta^2 + \dot{r}_z^2) + 2(\omega_0 + \alpha t)(\dot{r}_\eta r_z - r_\eta \dot{r}_z) + (\omega_0 + \alpha t)^2 (r_\eta^2 + r_z^2) \end{aligned} \tag{3.11}$$

With the help of equations (3 7), (3.5), (3.1), the first group of terms in equation (3.11) simplifies to

$$\dot{r}_\xi^2 + \dot{r}_\eta^2 + \dot{r}_z^2 = (x_1^2 + \dot{y}_1^2) + (x_1^2 + y_1^2)\,\theta^2 + 2(x_1\,\dot{y}_1 - y_1\,x_1)\,\dot{\theta} + u^2 + x_1^2\,x_1'^2 + y_1^2\,y_1'^2 + 2x_1\,y_1\,x_1'\dot{y}_1' - 2u(x_1\,\dot{x}_1' + y_1\,\dot{y}_1') \tag{3 12}$$

Ignoring axial inertia terms in the above

$$\dot{r}_\xi^2 + \dot{r}_\eta^2 + \dot{r}_z^2 = \dot{x}_1^2 + \dot{y}_1^2 + (x_1^2 + y_1^2)\,\dot{\theta}^2 \tag{3 13}$$

The second term in equation (3 11) represents Coriolis components and are neglected here The third group of terms in equation (3 11) represents the kinetic energy due to rotation which is

$$(\omega_0 + \alpha t)^2\,(r_\eta^2 + r_z^2) = (\omega_0 + \alpha t)^2 \left[\left\{ \eta + (y_1 + x_1\theta)\cos\phi - (x_1 - y_1\theta)\sin\phi \right\}^2 + \left\{ (R+z)u - x_1(x_1' - y_1\,\theta') - y_1(y_1' + x_1\,\theta') \right\}^2 \right] \tag{3 14}$$

Accounting for centrifugal components due to displacements of the particles on the line of centroid only, the above equation simplifies to

$$(\omega_0 + \alpha t)^2\,(r_\eta^2 + r_z^2) = (\omega_0 + \alpha t)^2 \left[2(R+z)u + y_1^2\cos^2\phi + x_1^2\sin^2\phi - x_1 y_1 \sin 2\phi \right] \tag{3 15}$$

Unaccounting for rigid body motion and neglecting u^2 terms, with the help of equations (3 13) and (3 15) the kinetic energy of the blade can be written as

$$T = \frac{1}{2}\int \rho v^2\,dA\,dz = \int_0^l \left[\frac{1}{2}\rho A\left(\dot{x}_1^2 + \dot{y}_1^2\right) + \frac{1}{2} I_{cg}\,\dot{\theta}^2 + (\omega_0 + \alpha t)^2\,(R+z)u\rho A + \frac{1}{2}(\omega + \alpha t)^2\,\rho A\left(y_1^2\cos^2\phi + x_1^2\sin^2\phi - x_1 y_1 \sin 2\phi\right) \right] dz \tag{3.16}$$

The total axial displacement, u at z due to bending is given by

$$u = -\int_0^z \frac{1}{2}\left(x_1'^2 + y_1'^2\right) dz \tag{3.17}$$

Hence, with the help of equations (3.17) and (3.1)

$$T = \rho \int_0^l A\left[\left(x + r_y\theta\right)^2 + \left(y - r_x\theta\right)^2\right] dz + \frac{1}{2}\int_0^l I_{cg}\dot{\theta}^2 dz$$
$$+ \frac{1}{2}\rho(\omega_0 + \alpha t)^2\left[-\int_0^l \left\{\left(x' + r_y'\theta + r_y\theta'\right)^2 + \left(y' - r_x'\theta - r_x\theta'\right)^2\right\}(R+z)dz\right.$$
$$\left. + \sin^2\phi \int_0^l A\left(x + r_y\theta\right)^2 dz + \cos^2\phi \int_0^l A\left(y - r_x\theta\right)^2 dz - \sin 2\phi \int_0^l A\left(x + r_y\theta\right)\left(y - r_x\theta\right)dz\right]$$

(3 18)

Using notation

$$\omega = \omega_0 + \alpha t \tag{3 19}$$

the kinetic energy can be written as

$$T = \frac{1}{2}\rho \int_0^l A\left[\left(\dot{x} + r_y\dot{\theta}\right)^2 + \left(\dot{y} - r_x\dot{\theta}\right)^2\right] dz + \frac{1}{2}\int_0^l I_{cg}\dot{\theta}^2 dz$$
$$+ \frac{1}{2}\rho\omega^2\left[-\int_0^l \left\{\left(x' + r_y'\theta + r_y\theta'\right)^2 + \left(y' - r_x'\theta - r_x\theta'\right)^2\right\}(R+z)dz\right.$$
$$\left. + \sin^2\phi \int_0^l A\left(x + r_y\theta\right)^2 dz + \cos^2\phi \int_0^l A\left(y - r_x\theta\right)^2 dz - \sin 2\phi \int_0^l A\left(x + r_y\theta\right)\left(y - r_x\theta\right)dz\right]$$

(3 20)

Reissner's Functional, which involves both the potential energy and complementary energy considerations and is known to yield simultaneously good stress and displacement fields, is employed along with the kinetic energy expression above to obtain the equations of motion for the blade The Reissner's functional is given by, [Dym and Shames (1973)],

$$I_R = \iiint_v \left[\tau_{ij}\varepsilon_{ij} - U^*\left(\tau_{ij}\right)\right] dv - \iiint_v B_i u_i \, dv - \iint_s T_i u_i \, ds \tag{3 21}$$

where

$\tau_{ij}\,\varepsilon_{ij}$ is the potential energy, $U^*\left(\tau_{ij}\right)$ is the complementary energy, B_i, T_i are the body and traction force terms respectively, u_i is the virtual displacement and v and s are the body volume and surface respectively.

The potential energy term, in the Reissner's functional is worked out to be

$$\iiint_v \tau_{ij}\varepsilon_{ij}dv = \int_0^l \iint_A [\tau_{zz}\varepsilon_{zz} + 2(\tau_{xz}\varepsilon_{xz} + \tau_{zy}\varepsilon_{zy})]dAdz$$
$$= \int_0^l (-M_y x'' - M_x y'' + T_\theta \theta'')dz \tag{3.22}$$

The complementary energy term is

$$\iiint_v U^*(\tau_{ij})dv = \iiint_v [\frac{t_{zz}^2}{2E} + \frac{t_{zx}^2 + t_{zy}^2}{2KG}]dv$$
$$= \int_0^l \left[\frac{M_x^2 I_{y_1y_1} + M_y^2 I_{x_1x_1} - 2M_x M_y I_{x_1y_1}}{2E(I_{y_1y_1}I_{x_1x_1} - I_{x_1y_1}^2)} + \frac{T_\theta^2}{2C}\right]dz \tag{3 23}$$

The body forces are assumed to be negligible i e

$$\iiint_v B_i u_i dv = 0. \tag{3.24}$$

Let the excitation forces on the blade be defined as components $F_x(z,t)$, $F_y(z,t)$ in the x and y directions and twisting moment $M(z,t)$. These forces are periodic with the nozzle passing frequency If n_z be the number of nozzles and ω the rotational frequency, the nozzle passing frequency is defined as

$$\nu = n_z\omega = n_s(\omega_0 + \alpha t) \tag{3 25}$$

The force components can be expressed in the form of Fourier series as

$$F_x(x,t) = a_{0x}(z) + \sum_m a_{mx}(z)\cos\left[mn_z\left(\omega_0 t + \frac{1}{2}\alpha t^2\right)\right] + \sum_m b_{mx}(z)\sin\left[mn_z\left(\omega_0 t + \frac{1}{2}\alpha t^2\right)\right]$$
$$F_y(y,t) = a_{0y}(z) + \sum_m a_{my}(z)\cos\left[mn_z\left(\omega_0 t + \frac{1}{2}\alpha t^2\right)\right] + \sum_m b_{my}(z)\sin\left[mn_z\left(\omega_0 t + \frac{1}{2}\alpha t^2\right)\right]$$
$$M(z,t) = a_{0M}(z) + \sum_m a_{mM}(z)\cos\left[mn_z\left(\omega_0 t + \frac{1}{2}\alpha t^2\right)\right] + \sum_m b_{mM}(z)\sin\left[mn_z\left(\omega_0 t + \frac{1}{2}\alpha t^2\right)\right]$$
(3 26)

where

$$a_{0x}(z)=\frac{\nu}{2\pi}\int_0^{2\pi/\nu}F_x(z,t)\,dt$$

$$a_{mx}(z)=\frac{\nu}{\pi}\int_0^{2\pi/\nu}F_x(z,t)\cos\left[mn_z\left(\omega_0 t+\frac{1}{2}\alpha t^2\right)\right]dt \qquad (3.27)$$

$$b_{mx}(z)=\frac{\nu}{\pi}\int_0^{2\pi/\nu}F_x(z,t)\sin\left[mn_z\left(\omega_0 t+\frac{1}{2}\alpha t^2\right)\right]dt$$

etc

Employing equations (3 20)-(3 24) and equation (3 26) the dynamic Reissner's functional can be written as

$$\begin{aligned}
L &= T - I_R \\
&= \frac{1}{2}\rho\int_0^l A\{(\dot{x}+r_y\theta)^2+(\dot{y}-r_x\dot{\theta})^2\}dz+\int_0^l I_{cg}\dot{\theta}^2\,dz \\
&+\frac{1}{2}\rho\omega^2\Bigg[-\int_0^l\left\{(x'+r_y\theta'+r_y'\theta)^2+(y'-r_x\theta'-r_x'\theta)^2\right\}(RI_1+I_2)dz \\
&+\sin^2\phi\int_0^l A(x+r_y\theta)^2\,dz+\cos^2\phi\int_0^l A(y-r_x\theta)^2\,dz]-\sin 2\phi\int_0^l A\left(x+r_y\theta\right)\left(y-r_x\theta\right)dz\Bigg] \\
&+\int_0^1\left[M_y x''+M_x y''-T_\theta\theta''+\frac{M_x^2 I_{y_1y_1}+M_y^2 I_{x_1x_1}-2M_xM_yI_{x_1y_1}}{2E(I_{y_1y_1}I_{x_1x_1}-I_{x_1y_1}^2)}-\frac{T_\theta^2}{2C}\right]dz \\
&+[a_{0x}(z)x+\sum_m a_{mx}(z)\cos\left[mn_z\left(\omega_0 t+\frac{1}{2}at^2\right)\right]x+\sum_m b_{mx}(z)\sin\left[mn_z\left(\omega_0 t+\frac{1}{2}at^2\right)\right]x \\
&+a_{0y}(z)y+\sum_m a_{my}(z)\cos\left[mn_z\left(\omega_0 t+\frac{1}{2}at^2\right)\right]y+\sum_m b_{my}(z)\sin\left[mn_z\left(\omega_0 t+\frac{1}{2}at^2\right)\right]y \\
&+a_{0M}(z)\theta+\sum_m a_{mM}(z)\cos\left[mn_z\left(\omega_0 t+\frac{1}{2}at^2\right)\right]\theta+\sum_m b_{mM}(z)\sin\left[mn_z\left(\omega_0 t+\frac{1}{2}at^2\right)\right]\theta]dz
\end{aligned} \qquad (3.28)$$

Using shape functions

$$\begin{aligned}
x&=\sum A_i(t)f_i(z) & M_x&=\sum D_i(t)h_i(z) \\
y&=\sum B_i(t)f_i(z) & M_y&=\sum E_i(t)h_i(z) \\
\theta&=\sum C_i(t)\bar{f}_i(z) & T_\theta&=\sum F_i(t)h_i(z)
\end{aligned} \qquad (3.29)$$

where

$$f_i(Z)=\frac{(i+2)(i+3)}{6}Z^{i+1}-\frac{i(i+3)}{3}Z^{i+2}+\frac{i(i+1)}{6}Z^{i+3}$$
$$\bar{f}_i(Z)=Z^i-\frac{i}{i+1}Z^{i+1}$$
$$h_i(Z)=\frac{(1-Z)^i}{i+1} \qquad (3\ 30)$$
$$Z=\frac{z}{l}$$

which satisfy the boundary conditions of a cantilever,

Ritz process

$$\frac{\partial L}{\partial A_i}=0 \quad \text{etc} \qquad (3\ 31)$$

is applied to the dynamic Reissner functional above to obtain the equations of motion

$$[M]\{\ddot{q}\}+[C]\{\dot{q}\}+[K]\{q\}=\{Q\}_0+\sum_m\{Q_m\}\cos mn_z\left(\omega_0 t+\frac{1}{2}at^2\right)$$
$$+\sum_m\{Q_{m+6}\}\sin mn_z\left(\omega_0 t+\frac{1}{2}at^2\right) \qquad (3\ 32)$$

The matrix elements have been described in the Appendix

The free vibration equation is solved computationally to obtain the natural frequencies and the eigenvector matrix *[U]*.

3.2 Response

Modal analysis technique is employed to obtain forced vibration response

Using

$$\{q\}=[U]\{h\} \qquad (3\ 33)$$

and premultiplying equation (3.32) by $[U]^T$ one gets

$$[\bar{M}]\{\ddot{h}\}+[\bar{C}]\{\dot{h}\}+[\bar{K}]\{h\}=\{Q\}_{0N}+\sum_m\{Q_m\}_N\cos mn_z\left(\omega_0 t+\frac{1}{2}at^2\right)$$
$$+\sum_m\{Q_{m+6}\}_N\sin mn_z\left(\omega_0 t+\frac{1}{2}at^2\right) \qquad (3.34)$$

where

$$
\begin{aligned}
&[\bar{M}] = [U]^T [M][U] \\
&[\bar{C}] = [U]^T [C][U] \\
&[\bar{K}] = [U]^T [K][U] \\
&\{Q\}_{0N} = [U]^T \{Q\}_0 \\
&\{Q_m\}_N = [U]^T \{Q_m\} \\
&\{Q_{m+6}\}_N = [U]^T \{Q_{m+6}\}
\end{aligned}
\tag{3 35}
$$

The decoupled kth modal equation can be readily written from the above as

$$
\begin{aligned}
M_k(\ddot{h}_k + 2x_k p_k \dot{h}_k + p_k^2 h_k) = Q_{0N_k} &+ \sum_m Q_{mN_k} \cos mn_z\left(\omega_0 t + \frac{1}{2}at^2\right) \\
&+ \sum_m Q_{(m+6)N_k} \sin mn_z\left(\omega_0 t + \frac{1}{2}at^2\right)
\end{aligned}
\tag{3 36}
$$

Defining the following non-dimensional parameters for the k th modal equation

$$
\begin{aligned}
&\tau_k = p_k t = \text{non - dimensional time} \\
&r_{0_k} = \frac{\omega_0}{p_k} = \text{initial frequency ratio} \\
&r_{i_k} = \frac{\omega}{p_k} = \text{instantaneous frequency ratio} \\
&r_{\alpha_k} = \frac{\alpha}{p_k^2} = \text{nondimensional sweep rate} \\
&H_k = \frac{\eta}{Q_{st_N}} = \text{ dynamic magnification factor (or displacenent ratio)} \\
&Q_{st_N} = \frac{Q_N}{M_k p_k^2} = \text{ static deflection}
\end{aligned}
\tag{3.37}
$$

equation (3.36) can be written as

$$
\begin{aligned}
\frac{d^2 H_k}{d\tau_k^2} + 2\varsigma_k \frac{dH_k}{d\tau_k} + H_k = Q_{st_{0N_k}} &+ \sum_m Q_{st_{mN_k}} \cos mn_z(r_0\tau + \frac{1}{2}r_\alpha \tau^2) \\
&+ \sum_m Q_{st_{(m+6)N_k}} \sin mn_z(r_0\tau + \frac{1}{2}r_\alpha \tau^2)
\end{aligned}
\tag{3.38}
$$

Equation (3 38) being linear the individual responses for the force harmonics can be calculated independently and then summed together to obtain the total response.

The response for the zeroth harmonic is, readily

$$H_{0k} = Q_{st0N_k} \tag{3.39}$$

while for the higher harmonics, the response, as in the earlier chapter can be written using Duhamel's Integral, as (for zero initial conditions)

$$\begin{aligned} H_{mk}(\tau) &= \int_0^{\tau} e^{-\zeta_k(\tau_k-\tau'_k)} \sin(\tau_k - \tau'_k)\cos mn_z\left(r_{0k}\tau'_k + \frac{1}{2}r_{\alpha k}\tau'^2_k\right) d\tau'_k \\ H_{(m+6)k}(\tau) &= \int_0^{\tau} e^{-\zeta_k(\tau_k-\tau'_k)} \sin(\tau_k - \tau'_k)\sin mn_z\left(r_{0k}\tau'_k + \frac{1}{2}r_{\alpha k}\tau'^2_k\right) d\tau'_k \end{aligned} \tag{3.40}$$

The nondimensional modal response from equations (3 39) and (3 40) above, can be processed along with equations (3 37), (3 33), (3 30) and (3 39) to obtain the blade displacement and moment fields Stresses are computed using Strength of Material formulae and the basic design stress is obtained by employing the von-Mises criterion on principal stresses

3.3 Results

A computer program, based on the above formulations, is developed for obtaining the forced vibration response of a turbine blade for step-up and step-down operations

Fig 3.4 shows a typical turbine blade, used in the present study for illustration The geometric and material properties of this blade are given in Table 3 1. The first five natural frequencies of the blade are listed in Table 3 2 Typical modal damping data and nozzle excitation for the blade have been shown in Figs (3.5) and (3.6) respectively These experimentally generated data have been taken from Vyas[1986] Fig 3 7 is the Campbell diagram for the blade, which defines the resonant speeds from the interaction of the blade natural modes and the excitation force harmonics (e g the interaction of the first blade mode with the first harmonic of the excitation force gives the resonant speed of 816 RPM, while the interaction of the first blade mode with the sixth harmonic of the excitation force gives the resonant speed of 135 RPM).

The program is illustrated for start up operation of the rotor from an initial speed of 0 RPM to a final speed of 4000 RPM. The blade stresses have been computed for the resonances occurring, in this speed range, due to the interaction between the first blade mode and first six harmonics of the nozzle excitation. The computation is illustrated for typical accelerations of 2000 RPM/min, 4000 RPM/min, 6000 RPM/min, 8000 RPM/min and 10000 RPM/min The effective nondimensional sweep rates $mn_z(\alpha / p_k^2)$, for these accelerations, fall in the range 1×10^{-4} to 5×10^{-3} (with $p_k = p_1 = 492.88$ Hz, $n_z = 36$, $m = 1,2.\ .6$).

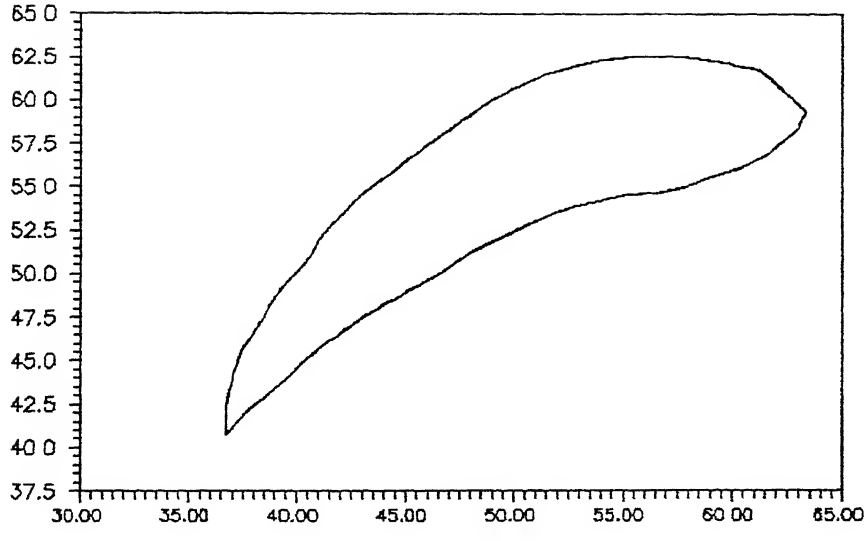

Fig. 3.4 Blade profile.

TABLE 3.1. Geometric & Material Properties of the Blade

Modulus of elasticity (E)		200 *GPa*
Modulus of rigidity (G)		*72 GPa*
Density (ρ)		8000 kg/m^3
Blade length		111 *mm*
Disc radius		180 *mm*
Pretwist angle		0 0 *rads*
Stagger angle		1 5708 *rads*
Area of cross section (A)		17 8447$\times 10^{-3}$ m^2
Moment of area about xx axis (I_{xx})	:	38 39254$\times 10^{-6}$ m^4
Moment of area about yy axis (I_{yy})	:	80 08938$\times 10^{-6}$ m^4
Moment of area about xy axis (I_{xy})	:	46 33235$\times 10^{-6}$ m^4
x co-ordinate of centre of flexture	:	27 45638 *mm*
y co-ordinate of centre of flexture		- 11.76078 *mm*

TABLE 3.2. Natural Frequencies for first 5 Modes.

MODE	*FREQUENCY (Hz)*
1	492.9
2	1767.0
3	3067.9
4	4180.0
5	8586.5

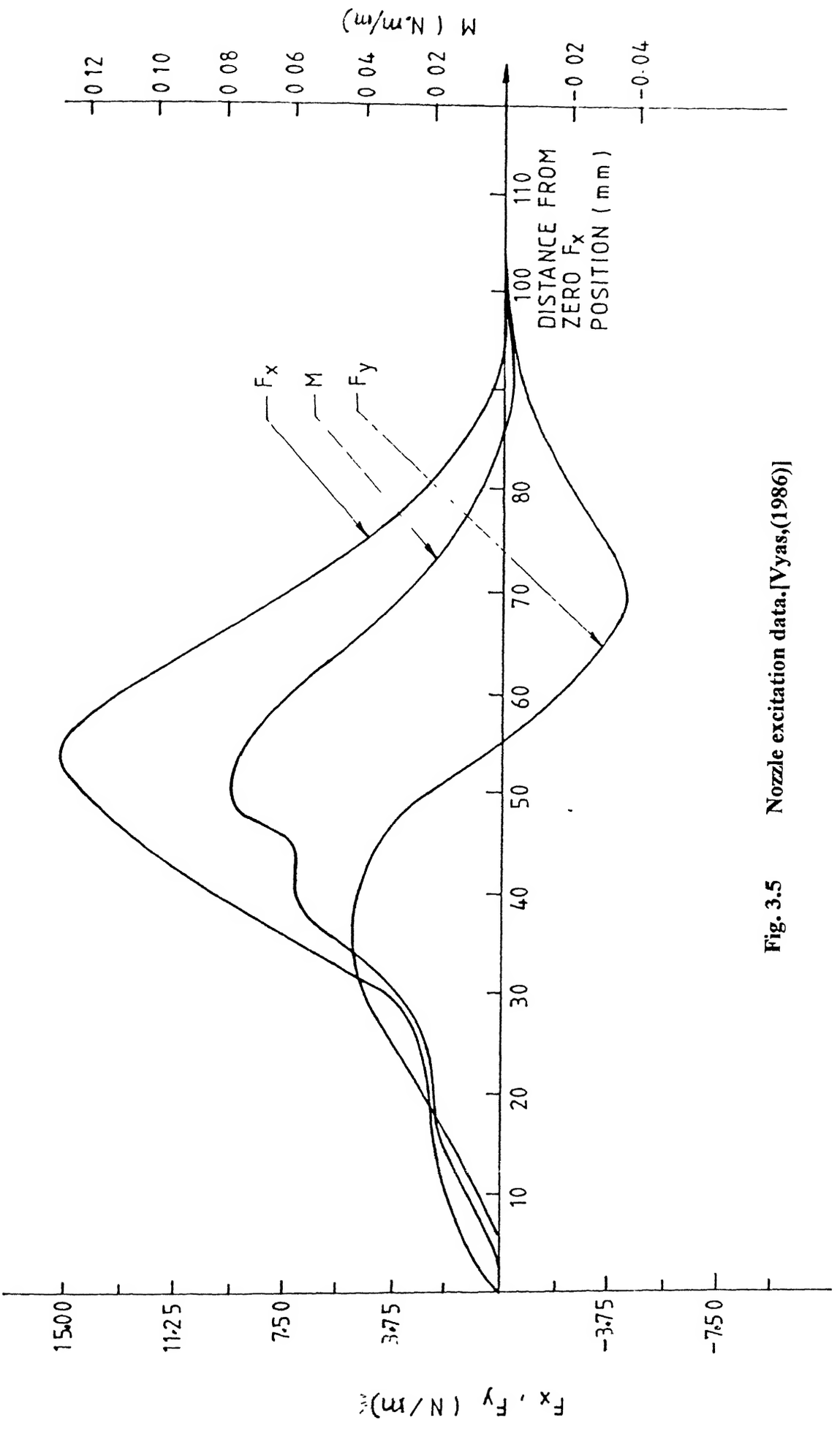

Fig. 3.5 Nozzle excitation data.[Vyas,(1986)]

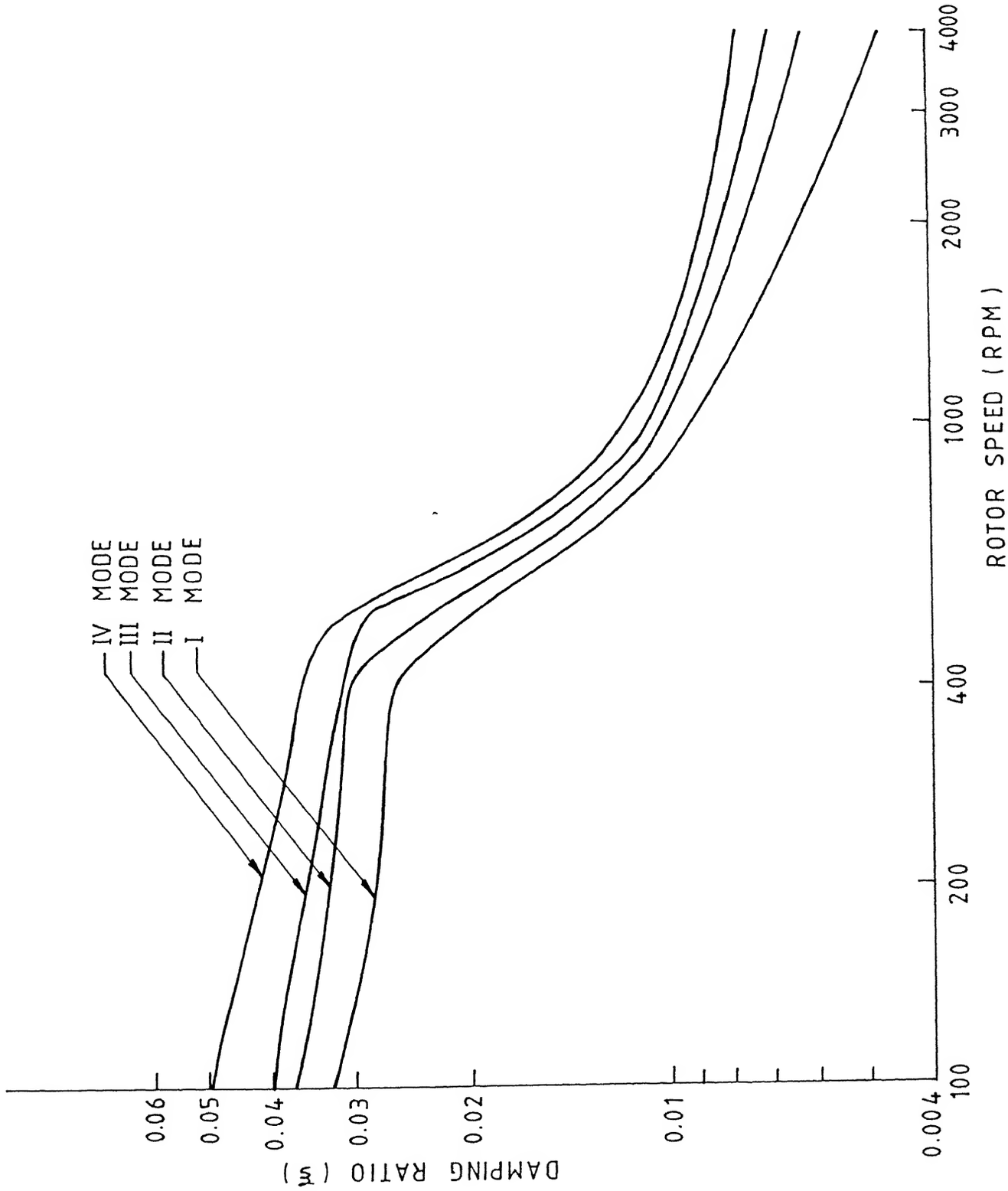

Fig. 3.6 Blade Damping data. [Vyas,(1986)]

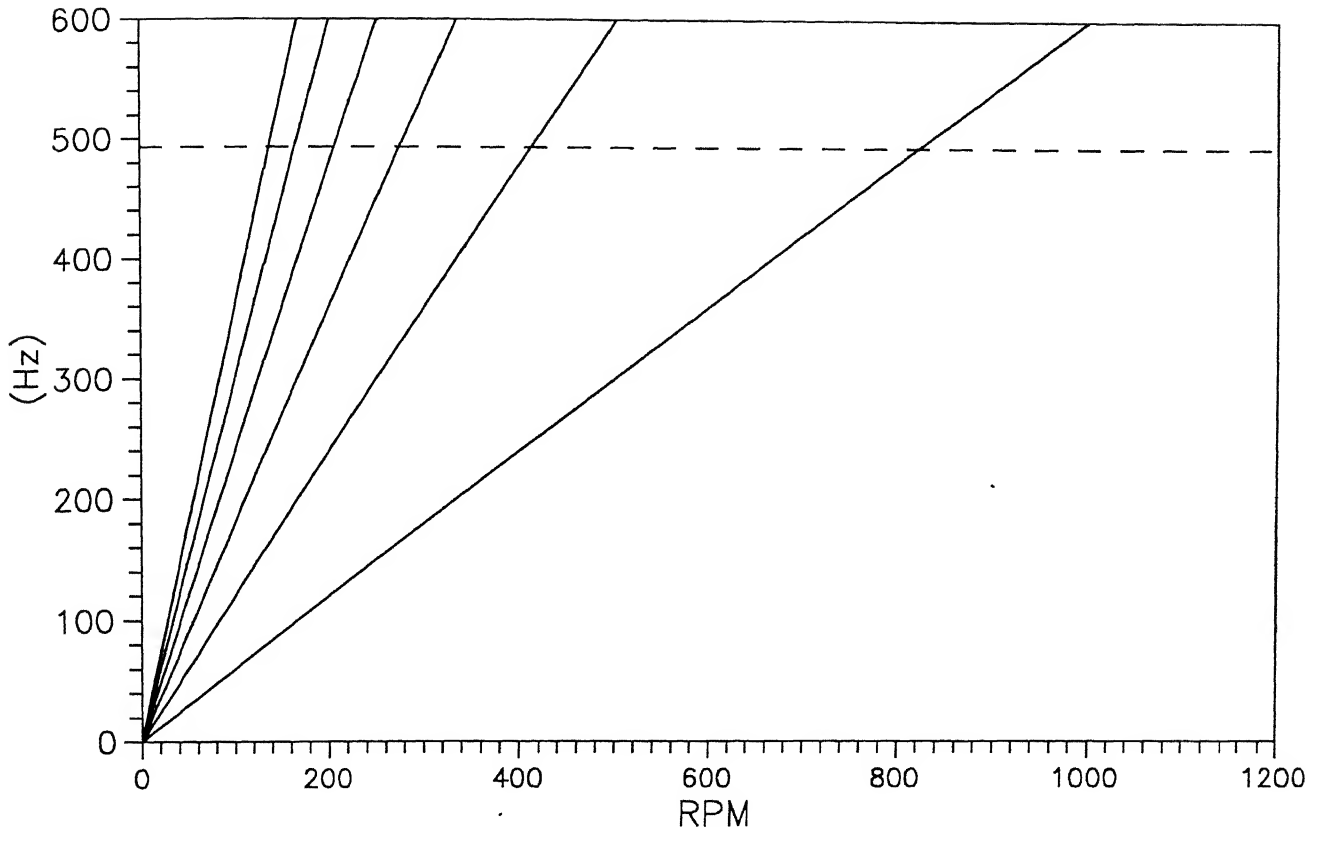

Fig. 3.7 Campbell diagram.

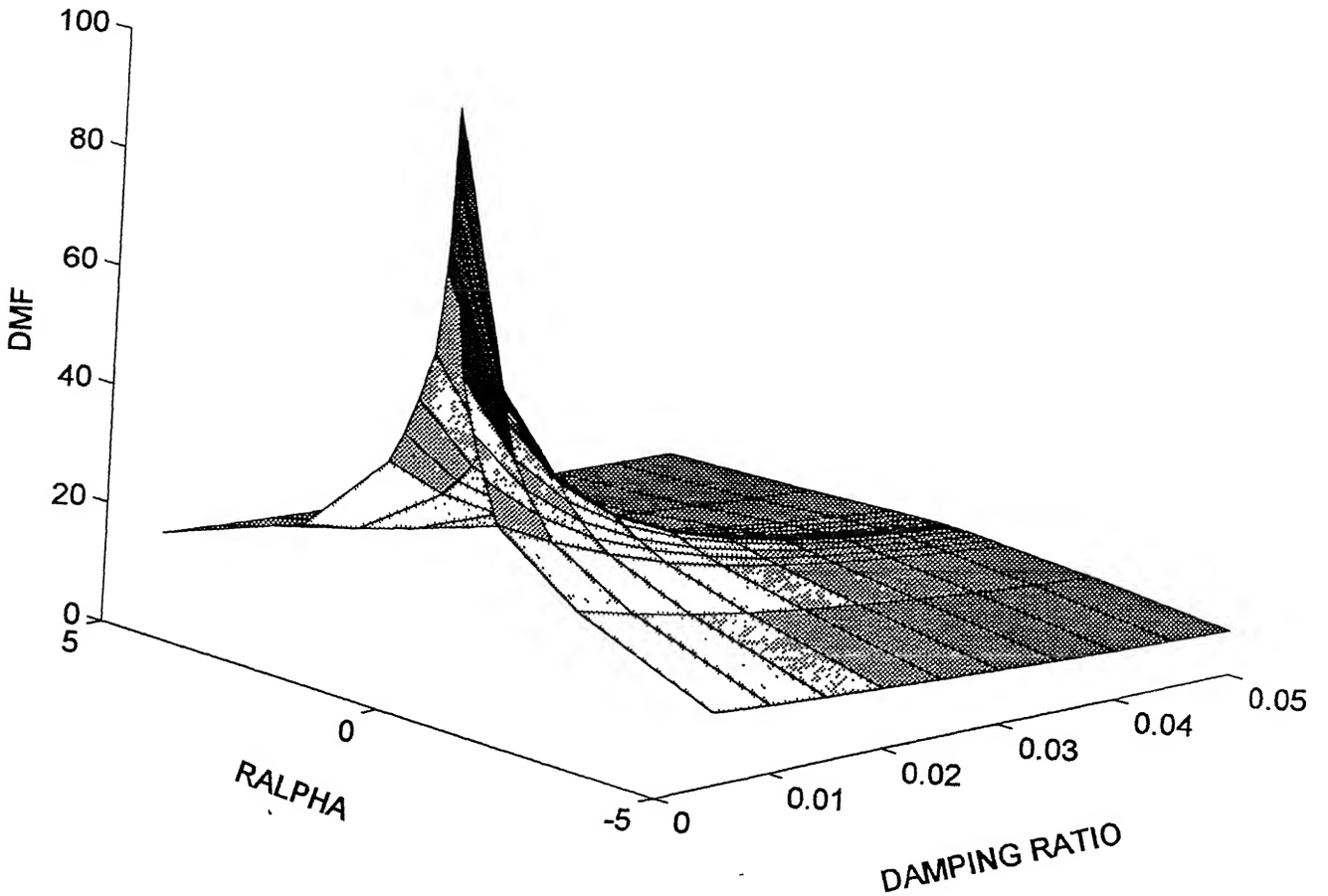

Fig. 3.8 **Non-dimensional peak transient response surface.**

TABLE 3.4 Transient Resonant Stresses

S.No	SPEED (RPM)	RESONANT STRESS (KPa)					
		Acceleration (RPM/min)					
		0.0	2000	4000	6000	8000	10000
1	135.830	1096.1	69.45	58.03	34.70	13.39	1.76
2	163.003	1166.3	96.21	61.43	51.66	30 35	12.51
3	203.758	1304.6	142.05	84.22	75.64	57.79	37.09
4	271.694	1299.6	160.03	90.41	78.95	75.55	60.38
5	407.617	1644.5	269.96	200.10	133.22	118.77	105.82
6	816.050	3087.1	913.59	772.45	676.39	578.48	481.14

For such small effective sweep rates, it is difficult to obtain a plot of the cyclic variation of the stress for the entire sweep range, as solutions required to be computed for very large number of points on the range However, from the design point of view , the excessive stresses incurred by the blade while passing through a resonant rotor speed would be of interest Therefore, for computational efficiency only the peak responses at the instances of momentary resonances are computed This is done, by employing the results obtained in nondimensional form for the case of a single degree of freedom system Comparison of the modal equation (3.38) of the blade with equation (2 5) of the previous chapter and between the blade modal response equations (3 40) with equation (2 7) reveals, that the results for the single degree freedom system can be readily extrapolated to obtain the blade modal response Fig 3 8 shows a nondimensional instantaneous peak response surface, plotted from the results of Table 2 1 The nondimensional peak response is plotted, in this figure, as function of the two parameters, namely sweep rate and damping This surface has been built into the computer program and the response peak response for the blade, for a given rate of acceleration, and given damping data, is directly read from the surface The blade stresses thus obtained at momentary resonances during the start-up operation, are listed in Table 3 3. It can be noted that the stress levels for lower sweep rates are higher, which is in consonance with the basic principles of the earlier chapter

3.4 Remarks

The computer program has been illustrated only for a start-up operation However, it is capable of handling shut-down operations (i e non-zero initial speeds and negative rates of acceleration) The peak stress level experienced by the blade, during a deceleration operation are not expected to be very different from the corresponding ones for positive acceleration, as can be seen from Table 2.1 of the previous chapter. The influence of initial speed on the peak response has not been, presently investigated However, the influence is not expected to be notable since the free vibration due to initial conditions is expected to wither away relatively fast.

CHAPTER 4

CONCLUSIONS

An attempt has been made in the present study to estimate the resonant stresses momentarily experienced by a turbine blade during a variable speed operation like start-up. The analytical formulation employs the Reissner's functional in conjunction with Ritz process to write the equations of motion The eigenvalue problem is solved to obtain the free vibration characteristics of the blade Modal analysis is used to process the equations of forced motion For a computationally efficient calculation of the modal peak responses, the nondimensional response data of the single degree freedom system is employed as a built-in data surface, in the blade program, whereby the blade modal responses are directly extrapolated from this surface The stress response of the blade is computed using Strength of Material formulae. The computer program developed on the basis of the analysis is illustrated for typical start-up operations.

Calculation of such transient resonant stresses is relevant for a blade designed to work satisfactorily at an innocuous constant speed for power generation, may fail entirely due to the fatigue damage cumulated through repeated infliction of high momentary resonant stresses, during every start-up or shut down operaration

As a next stage of analysis, fatigue damage calculations can be taken up. Cumulative fatigue theories, like the Miner's Rule in conjunction with familiar S-N diagrams or more advanced fracture mechanics principles, taking the transient resonant stresses as inputs, can be employed to attempt blade life predictions. The present analysis employs a nondimensional peak response data surface for efficient computation For fatigue life calculations, the envelope of the nondimensional response will be required to mark off time periods, during which the transient response is higher than some specified safe limit, say the endurance limit of the blade material. An approach to building such information within a life estimation software would be to set up an empirical relationship for the response envelope by applying an appropriate curve fitting algorithm on the data generated in the present study.

REFERENCES

Ansari, K A [1989], *' Turbine Blade Vibrations Review'*, Encyclopedia of Fluid Mechanics Vol Nicholas P Cherenisinoff Editor Gulf Publishing company, Texas, U S

Baker, J G [1939], *'Mathematical- Machine Determination of the Vibration of Accelerat Unbalanced Rotor'*, Journal of Applied Mechanics, Vol 6, pp.145-150

Banerjee, J R and Kennedy, D [1985], *' Response of Axially Loaded Timoshenko beams to Randc Loads'*, Journal of Sound and Vibration. 101(4), p 481.

Dym, C L and Shames, I H [1973], *'Solid Mechanics, A Variational Approach'*, McGraw H Publications

Fu-Sheng , C , et al [1981], *' Combined Friction in Material Damping of Resonant Steam Turbi Blade Response'*, ASME Paper No 81-DET-136

Griffin, J H [1980], *'Friction Damping of Resonant Stresses in Gas Turbine Engine Airfoil* Journal of Engg Power, ASME, Vol.102, p 329

Hiroyuki, K [1985], *'Non-Linear Vibrations of a Beam with a Mass Subjected to Alternati Electromagnetic Force'*, Bull JSME, Vol 28, No 237.

Hoyniak, D and Fleeter, S. [1981], *'Prediction of Aerodynamically Induced Vibrations Turbomachinary'*, Winter Annual Meeting of ASME, Nov, p 1.

Irretier, H. [1984], *'Numerical analysis of Transient Responses In Blade Dynamics'*, Vibrations Rot. Mach., Third International conference, University of York, England, p 255.

Jadwani, H M and Rao, J.S [1982], *'Forced Vibrations of Rotating Pretwisted Blades'*, Proceeding of IFToMM International Conference Rotor Dynamic Problems in Power Plants, p.259.

Jones, D I G [1977], *'Effect of Slip on Response of a Vibrating Compressor Blade'*, ASME 7 WA/GT-3

Leung, A.Y.T [1983], *' Dynamic Stiffness method for Exponentially Varying Harmonic Excitation continuous Systems'*, Journal of Sound and Vibration 98(3) p 337.

MacBain, J C [1976], *' Transient Response of a Cantilever Plate to Impact Using Hologra Interferometry and Finite Element Techniques'*, AFAPL-TR-76-56

Matsura, T. [1979], *' Blade Bending Vibrations Induced by Wakes'*, JMES, V-21, p 361

Plunkett, R. [1951], *' Free and Forced Vibration of Rotating Blades'*, Journal of Aero. Scie Vol 18, p 278

Rao, J S., et al [1978], *'Unsteady Forces- Blade Response'*, Project Report, ARDB, Ministry Defence, India

Rao, J S and Carnegie, W. [1972], *' Nonlinear Vibrations of Rotating Cantilever Beams Treatec Ritz Averaging Procedure'*, Journal of Royal Aero Society, Vol 76, p 566.

Rieger, N F [1994], *'Modern Technology Developments for Steam and Gas Turbine Bladi* Proceedings of IFToMM International Conference on Rotor Dynamics, p.17

Rieger, N F and Nowak, W J [1977], *' Analysis of Fatigue Stress in Turbine Blade Groups'*, EI Seminar on Steam Turbine Availability, Palo Alto, California

Salima, A L and Petyt, M [1978], *' Dynamic Response of Packets of Blades by the Finite Elem Method'*, Journal of Mechanical Design, Vol.100, p 660

Schnittger, J.R [1955], *' The Stress Problems of Vibrating Compressor Blades'*, Journal of Appl Mechanics, ASME, p 57

Sisto, F and Chang, A T [1981], *' The Influence of Gyroscopic Forces on the Dynamic Behavic of Rotating Blades'*, Proceedings of 5th Symp on Air Breathing Engines, Bangalore

Sisto, F., et al [1982], *' Blade Excitation due to Gyroscopic Forces'*, Proceedings of IFToM International Conference on Rotor Dynamic Problems in Power Plants, p.279.

Srinivasan, A V , et al [1978], *' Dynamic Analysis of an Assembly of Shrouded Blades Usi Component Modes'*, Journal of Mechanical Design, ASME, Vol 100, p.520.

Vyas, N S. [1986], *' Vibratory Stress Analysis and* Fatigue *Life Estimation of Turbine Blades'*, Ph. Thesis, I I.T., Delhi.

APPENDIX

The equation of motion for the turbomachine blade can be written in matrix form as

$$\begin{bmatrix} M_{11} & M_{12} & \cdots & \cdots & M_{16} \\ M_{21} & M_{22} & \cdots & \cdots & M_{26} \\ \vdots & & & & \vdots \\ \vdots & & & & \vdots \\ \vdots & & & & \vdots \\ M_{61} & M_{62} & \cdots & \cdots & M_{66} \end{bmatrix} \begin{Bmatrix} \ddot{A}_i \\ \ddot{B}_i \\ \vdots \\ \vdots \\ \vdots \\ \ddot{F}_i \end{Bmatrix} + \begin{bmatrix} K_{11} & K_{12} & \cdots & \cdots & K_{16} \\ K_{21} & K_{22} & \cdots & \cdots & K_{26} \\ \vdots & & & & \vdots \\ \vdots & & & & \vdots \\ \vdots & & & & \vdots \\ K_{61} & K_{62} & \cdots & \cdots & K_{66} \end{bmatrix} \begin{Bmatrix} A_i \\ B_i \\ \vdots \\ \vdots \\ \vdots \\ F_i \end{Bmatrix}$$

$$= \begin{Bmatrix} Q_{01} \\ Q_{02} \\ \vdots \\ \vdots \\ \vdots \\ Q_{06} \end{Bmatrix} + \sum_m \begin{Bmatrix} Q_{m1} \\ Q_{m2} \\ \vdots \\ \vdots \\ \vdots \\ Q_{m6} \end{Bmatrix} \cos m\upsilon t + \sum_m \begin{Bmatrix} Q_{m+6,1} \\ Q_{m+6,2} \\ \vdots \\ \vdots \\ \vdots \\ Q_{m+6,6} \end{Bmatrix} \sin m\upsilon t \qquad \text{(A.1)}$$

where the sub matrices-

$$M_{11} = \rho \int_0^l A f_i f_g \, dz$$

$$M_{13} = \rho \int_0^l A f_i f_g \, dz$$

$$M_{22} = \rho \int_0^l A f_i f_g \, dz$$

$$M_{23} = \rho \int_0^l A r_x g_i f_j \, dz$$

$$M_{31} = \rho \int_0^l A f_i r_y g_j \, dz$$

$$M_{32} = \rho \int_0^l A r_x f_i g_j \, dz$$

$$M_{33} = \rho \int_0^l \left[\rho A \left(r_x^2 + r_y^2 \right) + I_{cg} \right] g_i g_j \, dz$$

$$K_{11} = -\rho w^2 \left[-\int_0^l f_i' f_j' (RI_1 + I_2) dz + \sin^2 \phi \int_0^l A f_i f_j dz \right]$$

$$K_{12} = \frac{1}{2} \rho w^2 \sin 2\phi \int_0^l A f_i f_j dz$$

$$K_{13} = -\rho w^2 \left[-\int_0^l \left\{ \left(r_y' g_i + r_y g_i' \right) f_j \right\} (RI_1 + I_2) dz \right.$$

$$\left. + \sin^2 \phi \int_0^l A r_y g_i f_j dz + \frac{1}{2} \sin 2\phi \int_0^l A r_x g_i f_j dz \right]$$

$$K_{15} = -\int_0^l h_i f_j'' dz$$

$$K_{21} = \frac{1}{2} \rho w^2 \sin 2\phi \int_0^l A f_i f_j dz$$

$$K_{22} = -\rho w^2 \left[-\int_0^l f_i' f_j' (RI_1 + I_2) dz + \cos^2 \phi \int_0^l A f_i f_j dz \right]$$

$$K_{23} = -\rho w^2 \left[-\int_0^l \left\{ \left(r_x' g_i + r_x g_i' \right) f_j' \right\} (RI_1 + I_2) dz \right.$$

$$\left. - \cos^2 \phi \int_0^l A r_x g_i f_j dz - \frac{1}{2} \sin 2\phi \int_0^l A r_y g_i f_j dz \right]$$

$$K_{24} = -\int_0^l h_i f_j'' dz$$

$$K_{31} = -\rho w^2 \left[-\int_0^l \left\{ f_i' \left(r_y' g_j + r_y g_j' \right) \right\} (RI_1 + I_2) dz \right.$$

$$\left. + \sin^2 \phi \int_0^l A f_i r_y g_j dz + \frac{1}{2} \sin 2\phi \int_0^l A f_i r_x g_j dz \right]$$

$$K_{32} = -\rho w^2 \left[-\int_0^l \left\{ f_i' \left(r_x' g_j + r_x g_j' \right) \right\} (RI_1 + I_2) dz \right.$$

$$\left. - \cos^2 \phi \int_0^l A f_i r_x g_j f_i dz - \frac{1}{2} \sin 2\phi \int_0^l A f_i r_y g_j dz \right]$$

$$K_{33} = -\rho w^2 \left[-\int_0^l \left\{ \left(r_y' g_i + r_y g_i' \right)^2 - \left(r_x' g_i + r_x g_i' \right)^2 \right\} (RI_1 + I_2) dz \right.$$

$$\left. + \sin^2 \phi \int_0^l A r_y^2 g_i g_j dz + \cos^2 \phi \int_0^l A r_x^2 g_i g_j dz + \sin 2\phi \int_0^l A r_x g_i g_j dz \right]$$

$$K_{36} = \int_0^l h_i g_j' dz$$

$$K_{42} = -\int_0^l f_i' h_j dz$$

$$K_{44} = \int_0^l \frac{h_i h_j I_{y_1 y_1}}{E\left(I_{x_1 y_1}^2 - I_{x_1 x_1} I_{y_1 y_1}\right)} dz$$

$$K_{45} = \int_0^l \frac{h_i h_j I_{y_1 y_1}}{E\left(I_{x_1 y_1}^2 - I_{x_1 x_1} I_{y_1 y_1}\right)} dz$$

$$K_{51} = -\int_0^l f_i' h_j dz$$

$$K_{54} = \int_0^l \frac{h_i h_j I_{x_1 y_1}}{E\left(I_{x_1 y_1}^2 - I_{x_1 x_1} I_{y_1 y_1}\right)} dz$$

$$K_{55} = \int_0^l \frac{h_i h_j I_{x_1 y_1}}{E\left(I_{x_1 y_1}^2 - I_{x_1 x_1} I_{y_1 y_1}\right)} dz$$

$$K_{63} = \int_0^l g_i' h_j dz$$

$$K_{66} = -\int_0^l \frac{h_i h_j}{C} dz$$

$$Q_{01} = \int_0^l a_{0x} f_j dz \qquad Q_{m,1} = \int_o^l a_{mx} f_j dz \qquad Q_{m+6,1} = \int_o^l b_{mx} f_j dz$$

$$Q_{02} = \int_0^l a_{0y} f_j dz \qquad Q_{m,2} = \int_o^l a_{myx} f_j dz \qquad Q_{m+6,2} = \int_o^l b_{my} f_j dz$$

$$Q_{03} = \int_0^l a_{0M} g_j dz \qquad Q_{m,3} = \int_o^l a_{mM} g_j dz \qquad Q_{m+6,3} = \int_o^l b_{mM} g_j dz$$

(A-2)

All other elements are zero

$$\{q\}^T = \{A_i, B_i, C_i, D_i\} \tag{A-3}$$